

The Canada-France Redshift Survey XIII: The luminosity density and star-formation history of the Universe to $z \sim 1$

S. J. Lilly¹

Department of Astronomy, University of Toronto, 60 St George Street, Toronto, ON M5S 3H8,
Canada

O. Le Fèvre¹, F. Hammer¹

DAEC, Observatoire de Paris-Meudon, Place Jules-Janssen, 92195 Meudon, France

David Crampton¹

Dominion Astrophysical Observatory, West Saanich Road, Victoria, BC V8X 4M6, Canada

ABSTRACT

The comoving luminosity density of the Universe, $\mathcal{L}(\lambda)$ is estimated from the CFRS faint galaxy sample in three wavebands (2800 Å, 4400 Å and 1 μm) over the redshift range $0 < z < 1$. In all three wavebands, \mathcal{L} increases markedly with redshift. For a ($q_0 = 0.5, \Omega = 1.0$) cosmological model, the comoving luminosity density increases as $(1+z)^{2.1 \pm 0.5}$ at 1 μm, as $(1+z)^{2.7 \pm 0.5}$ at 4400 Å and as $(1+z)^{3.9 \pm 0.75}$ at 2800 Å, these exponents being reduced by 0.43 and 1.12 for (0.05,0.1) and (-0.85,0.1) cosmological models respectively. The $\mathcal{L}(\lambda) - \tau$ relation can be reasonably well modelled by an actively evolving stellar population with a Salpeter initial mass function (IMF) extending to $125 M_{\odot}$, and a star-formation rate declining as $\tau^{-2.5}$ with a turn-on of star-formation at early epochs. A Scalo (1986) IMF extending to the same mass limit produces too many long-lived low mass stars. This rapid evolution of the star-formation rate and comoving luminosity density of the Universe is in good agreement with the conclusions of Pei and Fall (1995) from their analysis of the evolving metallicity of the Universe. One consequence of this evolution is that the *physical* luminosity density at short wavelengths has probably declined by two orders of magnitude since $z \sim 1$.

Subject headings: galaxies: evolution cosmology: observations

1. INTRODUCTION

¹Visiting Astronomer, Canada-France-Hawaii Telescope, which is operated by the National Research Council of Canada, the Centre National de la Recherche Scientifique of France and the University of Hawaii

Recent deep redshift surveys, such as the Canada-France Redshift Survey (CFRS), have produced large samples of normal field galaxies at high redshifts out to $z > 1$. A great deal can be learnt about the evolution of galaxies from the study of these galaxies, both through the construction of distribution functions such as the luminosity function and through the detailed study of individual galaxies. However, for some purposes, it is of interest to study the integrated light from the whole population, i.e. the comoving luminosity density, $\mathcal{L}(\lambda, z)$. The principal motivation is that this quantity is independent of many of the details of galactic evolution and depends primarily on the global star-formation history of the Universe and the, possibly epoch-dependent, initial mass function (IMF) of the stars. In particular, $\mathcal{L}(\lambda, z)$ should be independent of the merging history of individual galaxies, and independent of the uncertainties concerning the comoving densities and timescales of rapidly evolving galaxies (i.e. whether a given object represents a short-lived evolutionary phase occurring in many galaxies or a longer duration phenomenon occurring in just a few).

Analysis of $\mathcal{L}(\lambda, z)$ thus offers the prospect of determining the global star-formation history of the Universe. It is reasonable to hope that the star-formation rate averaged over the entire galaxy population in the Universe might follow a relatively simple dependence on cosmic epoch, even if individual galaxies have more stochastic evolutionary histories. Other cases where the integrated comoving luminosity density of the Universe will be of interest include (a) the calculation of the change in the average metallicity in the Universe as sampled by quasar absorption lines (see e.g. Pei and Fall 1995); (b) the calculation of the expected rate of supernovae; and (c) the calculation of the closure mass-to-light ratio.

In this *Letter*, we construct the comoving luminosity density of the Universe at three wavelengths (2800 Å, 4400 Å, and 1 μm), over the redshift interval $0 < z < 1$, from the CFRS galaxy sample. We consider three representative cosmological models: ($q_0 = 0.5, \Omega_0 = 1$) and (0.05, 0.1) Friedman models, and a low density zero-curvature model, (-0.85, 0.1). We take $H_0 = 50h_{50} \text{ kms}^{-1}\text{Mpc}^{-1}$ in computing volume elements.

2. CONSTRUCTION OF THE COMOVING LUMINOSITY DENSITY

2.1. Estimation of the $0.2 < z < 1.0$ luminosity density from the CFRS

The CFRS galaxy sample has been described in detail elsewhere (Lilly et al. 1995a, Le Fèvre et al. 1995a, Lilly et al. 1995b, Hammer et al. 1995, and Crampton et al. 1995; CFRS V). It consists of 730 *I*-band selected galaxies ($17.5 < I_{AB} < 22.5$), of which 591 (i.e. more than 80%) have secure redshifts in the range $0 < z < 1.3$, with a median $\langle z \rangle \sim 0.56$. All objects have *V* and *I* photometry, and most have also been observed in *B* and *K*, allowing the spectral energy distribution to be defined over a long wavelength baseline. Scientific analyses relevant to the

subject of this *Letter* include analysis of the luminosity function (Lilly et al. 1995c; CFRS VI), spatial correlation function (Le Fevre et al. 1996) and galaxy morphologies (Schade et al 1995).

The contribution to the comoving luminosity density from directly observed sources may be easily estimated using the V_{max} formalism used to construct the luminosity function (see CFRS VI).

$$\mathcal{L}(\lambda) = \sum_i \frac{L_i(\lambda)}{V_{max,i}}$$

with $V_{max,i}$ for each galaxy, i , defined and computed as in CFRS VI. The luminosity density has been computed at rest-4400 Å, rest-2800 Å and rest-1 μm. The estimates of $L_i(\lambda)$ are thus *interpolations* of our available *BVIK* photometry, except for the rest-2800 Å estimate which is a modest extrapolation for $z < 0.5$. The spectral energy distributions (SEDs) for individual galaxies are interpolated from the four SEDs given by Coleman et al. (1980; CWW) so as to match the observed colors of each galaxy.

One source of uncertainty arises from our failure to obtain secure redshift identifications for 19% of the galaxies. The likely nature of these galaxies is discussed in CFRS V. In computing the luminosity density, we have assigned all of the unidentified galaxies a redshift based on their photometric properties. This procedure introduces a maximum 10% uncertainty in \mathcal{L} over the $0.2 < z < 1.0$ range. The uncertainty at the extremes of the CFRS $N(z)$, at $z < 0.2$ and $z > 1.0$, is obviously larger, and we do not present the luminosity density in these redshift regimes. Our uncertainty in $\mathcal{L}(\lambda)$ is estimated from the sum in quadrature of the bootstrap error obtained by resampling the sample (see CFRS VI), the 10% error arising from the spectroscopic incompleteness, plus a Poisson error of $(2.5/N)^{0.5}$ which reflects the fact that galaxies are clustered in redshift space (see CFRS VI and CFRS VIII). We refer to the luminosity densities derived in this way as the “directly observed” luminosity densities. They are listed in Table 1 in units of $h_{50}^{-2} \text{WHZ}^{-1} \text{Mpc}^{-3}$. For reference, the Sun has $L(4400) = 3.4 \times 10^{11} \text{WHZ}^{-1}$ and one present-day L* galaxy ($M_{AB}(B) = -21.0 + 5 \log h_{50}$) per Mpc^{-3} produces a luminosity density of $1.14 \times 10^{22} h_{50}^{-2} \text{WHZ}^{-1} \text{Mpc}^{-3}$.

A second major uncertainty is the contribution from galaxies whose individual luminosities place them below the magnitude limit of the CFRS sample. We have approached this problem by fitting the rest- B luminosity functions of blue and red galaxies, as derived in different redshift intervals in CFRS VI, and integrating these over all luminosities to produce the luminosity density in the rest-frame B -band. The luminosity function of red and blue populations are assumed to have constant shape ($\alpha = -1.3$ for blue and $\alpha = -0.5$ for red) but a normalization in both M^* and ϕ^* that varies with epoch. As seen in Table 1, the increase in this “LF-estimated” luminosity density over that “directly-observed” in the CFRS galaxies is modest at $z < 0.75$, but quite large (a factor of about two) for $0.75 < z < 1.0$. A formal uncertainty in this procedure was estimated by considering the range of (M^*, ϕ^*) values that gave acceptable fits to the observed luminosity

function, but this estimate is unrealistically small, so a 1σ uncertainty of 33% of the additional flux was adopted (i.e. providing a $\pm 1\sigma$ range of a factor of two in the additional flux). Luminosity densities at the other wavelengths were then produced by applying luminosity-weighted average colors, $(2800 - 4400)_{AB}$ and $(4400 - 10000)_{AB}$, derived from the “directly-observed” CFRS galaxies.

2.2. The local luminosity density

There have been several recent determination of the local luminosity function based on surveys of several thousand galaxies. Converting the photometric systems as best we can (some are quite poorly defined) and integrating the luminosity functions we obtain values of $\log(L(4400))$ (with the same units as above) of 19.30 (Loveday et al. 1992), 19.40 (da Costa et al. 1994), 19.55 (Marzke 1994a) and 19.22 (Marzke 1994b). The r -selected luminosity function of Lin et al. (1995) gives 19.24 if the average $(B - r) \sim 1.0$. A simple average of all of the above gives 19.34 ± 0.06 and the Loveday (1992) value, 19.30, was finally adopted, with an uncertainty of 0.1 in the log. The local luminosity densities at 2800 \AA and $1 \mu\text{m}$ have been estimated by applying luminosity weighted colours to the B -band luminosity density. These colors were estimated using the CWW SEDs from the Marzke et al. (1994b) morphological type-dependent luminosity function and from the Metcalfe et al. (1991) (B-V)-dependent luminosity function. These two estimates agree to within 0.15 in the (4400-10000) color and to within 0.3 in the (2800-4400) color and We assign uncertainties of 0.20 and 0.10 in the log to the estimates of the local luminosity density at 2800 \AA and $1 \mu\text{m}$ (see Table 1).

3. THE EVOLUTION OF THE LUMINOSITY DENSITY

3.1. Parameterization as $(1 + z)^\alpha$

As shown in Figure 1, the “LF-estimated” luminosity densities are well-represented by power-laws in $(1 + z)$. If we write $\mathcal{L}(\lambda, z) = \mathcal{L}_0(\lambda)(1 + z)^{\alpha(\lambda)}$ then we find $\alpha(2800) = 3.90 \pm 0.75$, $\alpha(4400) = 2.72 \pm 0.5$, and $\alpha(10000) = 2.11 \pm 0.5$ for the (0.5,1.0) cosmology as plotted on the Figure. Changing to $q_0 = 0.0$ introduces an offset exactly equal to $0.5 \log(1 + z)$. The lowest panel in Figure 1 shows that in the two alternative cosmological models considered, (0.05,0.1) and (-0.85,0.1), the slopes would be decreased by approximately 0.43 and 1.12 respectively.

3.2. Parameterization with epoch

In terms of stellar populations, it is of interest to plot these changing luminosity densities as a function of cosmic epoch. In view of the uncertainty in both H_0 and q_0 , and since we wish to compare the evolving luminosity densities with stellar population models, a reasonable approach is to normalize the present age of the Universe to 15 Gyrs, as representative of the age of the oldest stellar populations. This therefore implies values of H_0 of 45, 60 and 85 $\text{kms}^{-1}\text{Mpc}^{-1}$ for the (0.5,1.0), (0.05,0.1) and (-0.85,1.0) cosmologies respectively.

The upper panel of Figure 2 shows the comoving luminosity densities as a function of epoch. For simplicity, the $L(\lambda)$ have been transcribed from Figure 1 *without* correction for the different *volume elements* implied by these different values of H_0 . Straight lines have been fit to the data for each cosmological model, and the gradients, $d(\log\mathcal{L}(\lambda))/dt$, are listed in Table 2. The variation of $\mathcal{L}(\lambda)$ is almost independent of q_0 , especially for the zero- λ models and the longer wavelengths (4400 Å and 1 μm). The luminosity density declines faster than expected for the purely passive evolution of an old stellar population, by which we mean the evolution (due to main-sequence burn-down) of a stellar population that has no continuing star-formation after an initial burst. In their comparison of models, Charlot, Worthey and Bressan (1996) find, with a Salpeter IMF and solar metallicity, $d(\log\mathcal{L}(4400))/dt = 0.042 \pm 0.008$ and $d(\log\mathcal{L}(22000))/dt = 0.029 \pm 0.006$ for ages between 5-17 Gyr, about a half of what is observed.

3.3. Towards a global history of star-formation?

An interesting question arises as to whether a simple model, defined by a time-dependent star-formation rate and a time-independent initial mass function, can, ignoring the effects of reddening by dust, reproduce the form of Figure 2. A preliminary investigation suggests that the answer is probably “yes”, provided that the IMF is reasonably rich in massive stars. In the two lower panels of Figure 2 two sets of simple models, generated from the GISSEL library (Bruzual and Charlot 1992), are compared with our data. The middle panel shows model stellar populations with the Salpeter power-law IMF (with $x = 1.35$) with $0.1 M_\odot < M < 125M_\odot$ that reproduce the $\mathcal{L}(2800)$ over the redshift range $0 < z < 1$. Since the light at 2800 Å is dominated by very young stars with this IMF, the models are required to have a time-dependent star-formation rate proportional to $\tau^{-2.5}$ over the relevant range of epochs (or slightly steeper, τ^{-3} , for the (0.05,0.1) cosmology). The four models shown in the middle panel all share this $\tau^{-2.5}$ star formation history but have a turn-on of star-formation 2,3,4 and 5 Gyr after the Big Bang. A model starting 2 to 3 Gyr after the Big Bang would clearly give a reasonable representation of the data, given the uncertainties in both data and models. The gradients in $\mathcal{L}(\lambda, \tau)$ and the 15 Gyr colors of the 3 Gyr model are listed in Table 2.

Initial mass functions which are less rich in massive stars do less well. In the lower panel of Figure 2, the predictions of similar models based on the Scalo (1986) IMF, which has almost an order of magnitude fewer high mass stars relative to solar mass stars, are shown. To match the ultraviolet luminosity density, the star-formation rate is set to $\tau^{-2.8}$, but the models are otherwise similar to those shown in the middle panel. These models all produce too much long wavelength light (i.e. at 4400 Å and at 1 μm) by the present epoch and/or do not decline in brightness at the longer wavelengths fast enough because of the large number of solar mass stars produced in the star-formation activity required to yield the high ultraviolet $\mathcal{L}(2800)$ at high redshifts. The adoption of the (-0.85,0.1) cosmology would alleviate this problem by reducing the required evolutionary gradient at 1 μm. However, uncertainties in the stellar models (e.g. see Charlot, Worthey and Bressan 1996) are still large enough to suggest that these conclusions concerning the IMF should be treated with caution.

The above analysis has ignored the effects of reddening due to dust (as well as other metallicity related effects in the models). If the effect of dust was independent of epoch, then it would simply shift the long wavelength curves of each model to higher values (since the models are normalized to the observed $\mathcal{L}(2800)$), thus exacerbating the problem with the Scalo IMF.

4. DISCUSSION AND SUMMARY

Analysis of the CFRS galaxy sample indicates that the observed luminosity density of the Universe in the ultraviolet, optical and near-infrared wavebands increases markedly with redshift over $0 < z < 1$, as $\mathcal{L} \propto (1+z)^{2.1 \pm 0.5}$ at 1 μm, $\mathcal{L} \propto (1+z)^{2.7 \pm 0.5}$ at 4400 Å and $\mathcal{L} \propto (1+z)^{3.9 \pm 0.75}$ at 2800 Å, for the (0.5,1.0) cosmology. The exponents would be reduced by 0.43 and 1.12 for (0.05,0.1) and (-0.85,0.1) cosmological models respectively. If an IMF rich in massive stars is assumed (as seems to be required) and if the effects of dust are ignored, then the ultraviolet luminosity density translates more or less directly to the star-formation rate, implying a rapid decline in the overall star-formation rate since $z \sim 1$.

At $z \sim 1$, the global star-formation rate was a factor of 15 higher for (0.5,1.0), 11 times higher for (0.05,0.1) and 7 times higher for (-0.85,0.1), with an uncertainty in each case of about 0.22 in the log. These large increases are in remarkably good agreement with the quite independent estimates of Pei and Fall (1995), a factor of 20 increase for (0.5,1.0) and of 10 for (0.0,0.0), based on a careful modelling of the change in mean metallicity of the Universe.

The *physical* luminosity density at 2800 Å has evidently declined as $(1+z)^{6.7 \pm 0.75}$ for a (0.5,1.0) cosmological model, i.e. by a factor of 60-170 since $z \sim 1$. This large factor is reduced by only a factor of two even in the extreme (-0.85,0.1) model.

We were initially encouraged to compute the luminosity density by Mike Fall, and we have

greatly benefitted from several subsequent discussions with him and with Ray Carlberg. SJL's research is supported by the NSERC of Canada and the CFRS project has been facilitated by a travel grant from NATO.

REFERENCES

- Charlot, S., Bruzual, G.A., 1993, ApJ, 405, 538
- Charlot, S., Worthey, G., Bressan, P., 1986, ApJ, *in press*.
- Coleman, G.D., Wu, C.C., Weedman, D.W., 1980, ApJ(Supp), 43, 393 (CWW)
- Crampton, D., Le Fèvre, O., Lilly, S.J., Hammer, F., 1995, ApJ, 455, 96 (CFRS V)
- Da Costa, L.N., Geller, M.J., Pellegrini, P.S., Latham, D.W., Fairall, A.P., Marzke, R.O., Willmer, C.N.A., Huchra, J.P., Calderon, J.H. Ramella, M., Kurtz, M.J.; 1994, ApJ(Letter), 424, L1.
- Hammer, F., Crampton. D., Le Fèvre, O., Lilly, S.J., 1995a, ApJ, 455, 88
- Le Fèvre, O., Crampton. D., Lilly, S.J., Hammer, F., Tresse, L., 1995, ApJ, 455, 60
- Le Fèvre, O., Hudon, D., Lilly, S.J., Crampton. D., Hammer, F., 1996, ApJ, in press.
- Lilly, S.J., Le Fèvre, O., Crampton. D., Hammer, F., Tresse, L., 1995a, ApJ, 455, 50
- Lilly, S.J., Hammer, F., Le Fèvre, O., Crampton. D., 1995b, ApJ, 455, 75
- Lilly, S.J., Tresse, L., Hammer, F., Crampton, D., Le Fèvre, O.,; 1995c, ApJ, 455, 108 (CFRS VI)
- Lin, H., Kirshner, R.P., Shectman, S.A., Landry, S.D., Oemler, A., Tucker, D.L., Schechter, P.L.; 1996, ApJ, submitted.
- Loveday, J., Peterson, B.A., Efstathiou, G., Maddox, S.J., 1992, ApJ, 390, 338
- Marzke, R.O., Geller, M.J., Huchra, J.P., Corwin, H., 1994a, ApJ 428, 43
- Marzke, R.O., Geller, M.J., Huchra, J.P., Corwin, H., 1994b, AJ 108, 437
- Metcalfe, N., Shanks, T., Fong, R., Jones, L.R, 1991, MNRAS, 249, 498
- Pei, Y.C., Fall, S.M., 1995, ApJ, 454, 69
- Schade, D.J., Lilly, S.J., Crampton, D., Hammer, F., Le Fèvre, O., Tresse, L., 1995, ApJLett, 451, L1

Fig. 1.— The comoving luminosity density ($\text{WHz}^{-1}\text{Mpc}^{-3}$) of the Universe in three wavebands. The small symbols at $z > 0.2$ are the “directly-observed” luminosity density, the larger symbols with error bars are the “LF-estimated” luminosity density (see text). The population of galaxies redder than Sbc are shown as squares, those bluer than Sbc as open circles and that of all galaxies as solid circles. The solid line shows the best-fit power-laws for the “LF-estimated” luminosity density for “all” galaxies in each waveband. The luminosity densities are calculated for the (0.5,1.0) cosmological model. The panel at bottom shows the roughly linear offset that should be applied for the (0.05,0.1) and (-0.85,0.1) cosmological models.

Fig. 2.— The comoving “LF-estimated” luminosity density for “all” galaxies from Figure 1, plotted as a function of epoch. The epoch is normalized so that the present epoch is 15 Gyr, irrespective of the cosmological model (see text). In the upper panel, straight lines have been fit to the data for each cosmological model. The solid circles and solid line represent the (0.5,1.0) cosmological model, open squares and dashed line, the (0.05,0.1) model, and the triangles and dotted line, the (-0.85,0.1) model. The dashed curve in the upper panel labelled CWB is the passively evolving model of Charlot et al. (1996). The same data points are reproduced on the two lower panels. The middle panel shows stellar population models with a Salpeter initial mass function, the bottom panel shows models with a Scalo (1986) initial mass function, in both cases the IMF extends over the range $0.1M_{\odot} < M < 125M_{\odot}$. In each case, four models are shown which have the same star-formation history ($\propto \tau^{-2.5}$ with the Salpeter IMF, $\propto \tau^{-2.8}$ with the Scalo IMF) but different turn-ons at 2, 3, 4, and 5 Gyr.

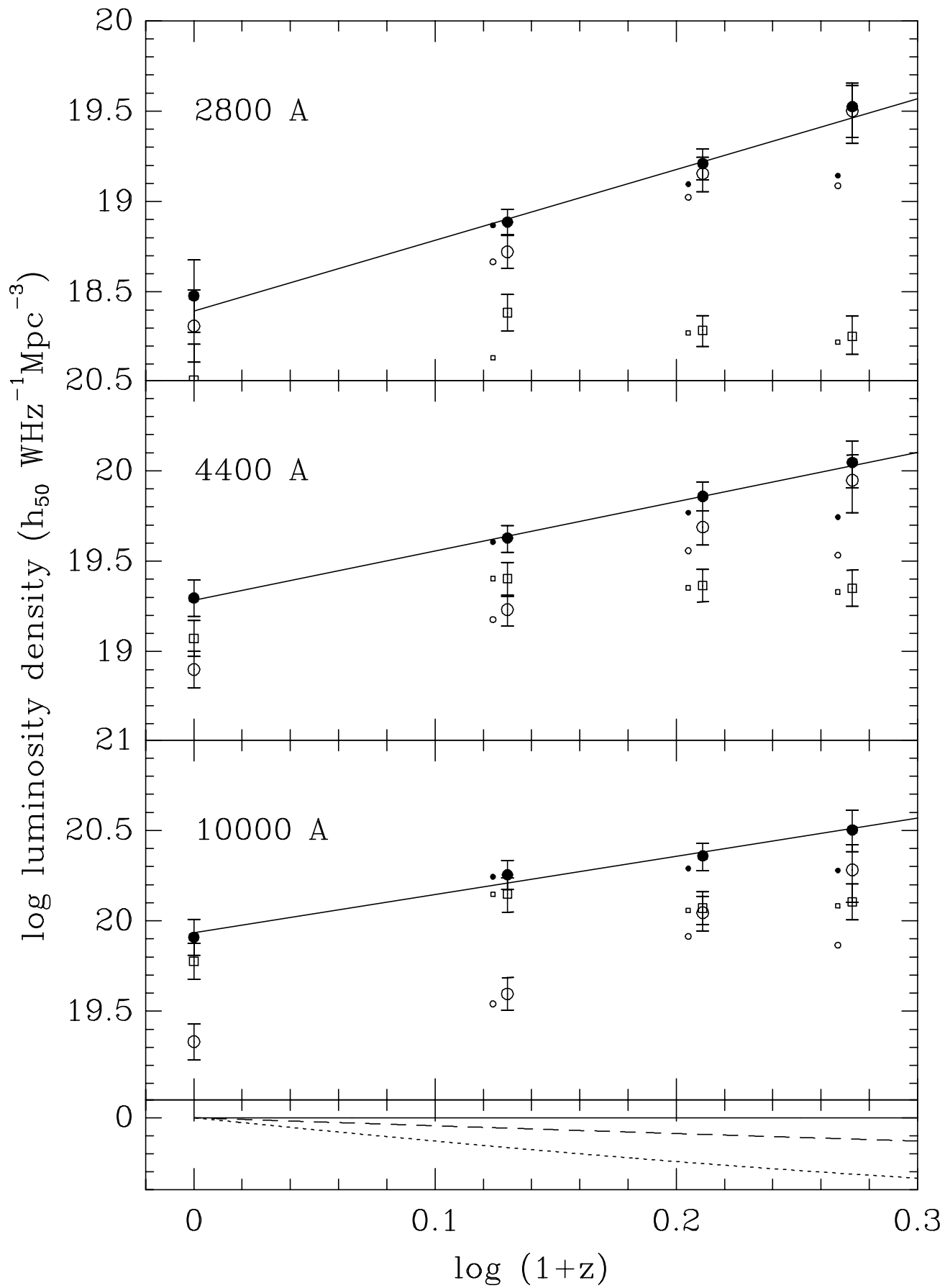


TABLE 1
ESTIMATES OF THE COMOVING LUMINOSITY DENSITY

sample ^a	redshift	2800 Å ^b	4400 Å ^b	1 μm ^b
“Directly observed”				
blue	0.20-0.50	18.666±0.08	19.177±0.08	19.541±0.08
	0.50-0.75	19.024±0.08	19.558±0.08	19.914±0.08
	0.75-1.00	19.087±0.08	19.533±0.08	19.866±0.08
red	0.20-0.50	18.135±0.10	19.404±0.09	20.148±0.09
	0.50-0.75	18.274±0.08	19.353±0.09	20.058±0.09
	0.75-1.00	18.222±0.11	19.330±0.10	20.084±0.10
all	0.20-0.50	18.868±0.07	19.606±0.07	20.244±0.08
	0.50-0.75	19.096±0.07	19.769±0.07	20.290±0.07
	0.75-1.00	19.143±0.07	19.744±0.07	20.279±0.07
“LF-estimated”				
blue	local ^d	18.311±0.20	18.901±0.10	19.331±0.10
	0.20-0.50	18.722±0.08	19.232±0.08	19.596±0.09
	0.50-0.75	19.155±0.09	19.689±0.09	20.045±0.09
	0.75-1.00	19.502±0.16	19.948±0.16	20.282±0.16
red	local ^d	18.011±0.20	19.073±0.10	19.776±0.10
	0.20-0.50	18.385±0.10	19.404±0.09	20.148±0.09
	0.50-0.75	18.288±0.08	19.365±0.09	20.071±0.09
	0.75-1.00	18.255±0.11	19.351±0.10	20.105±0.10
all	local ^c	18.478±0.20	19.296±0.10	19.909±0.10
	0.20-0.50	18.886±0.07	19.628±0.07	20.255±0.08
	0.50-0.75	19.210±0.08	19.858±0.08	20.359±0.07
	0.75-1.00	19.525±0.15	20.046±0.13	20.503±0.11

^awhether the galaxies are intrinsically bluer or redder than a present-day Sbc galaxy

^blog luminosity density in units of $h_{50} \text{ WHz}^{-1} \text{ Mpc}^{-3}$

^cfrom Loveday et al (1992) - see text for discussion.

^destimated from *B*-band luminosity data and average colors - see text.

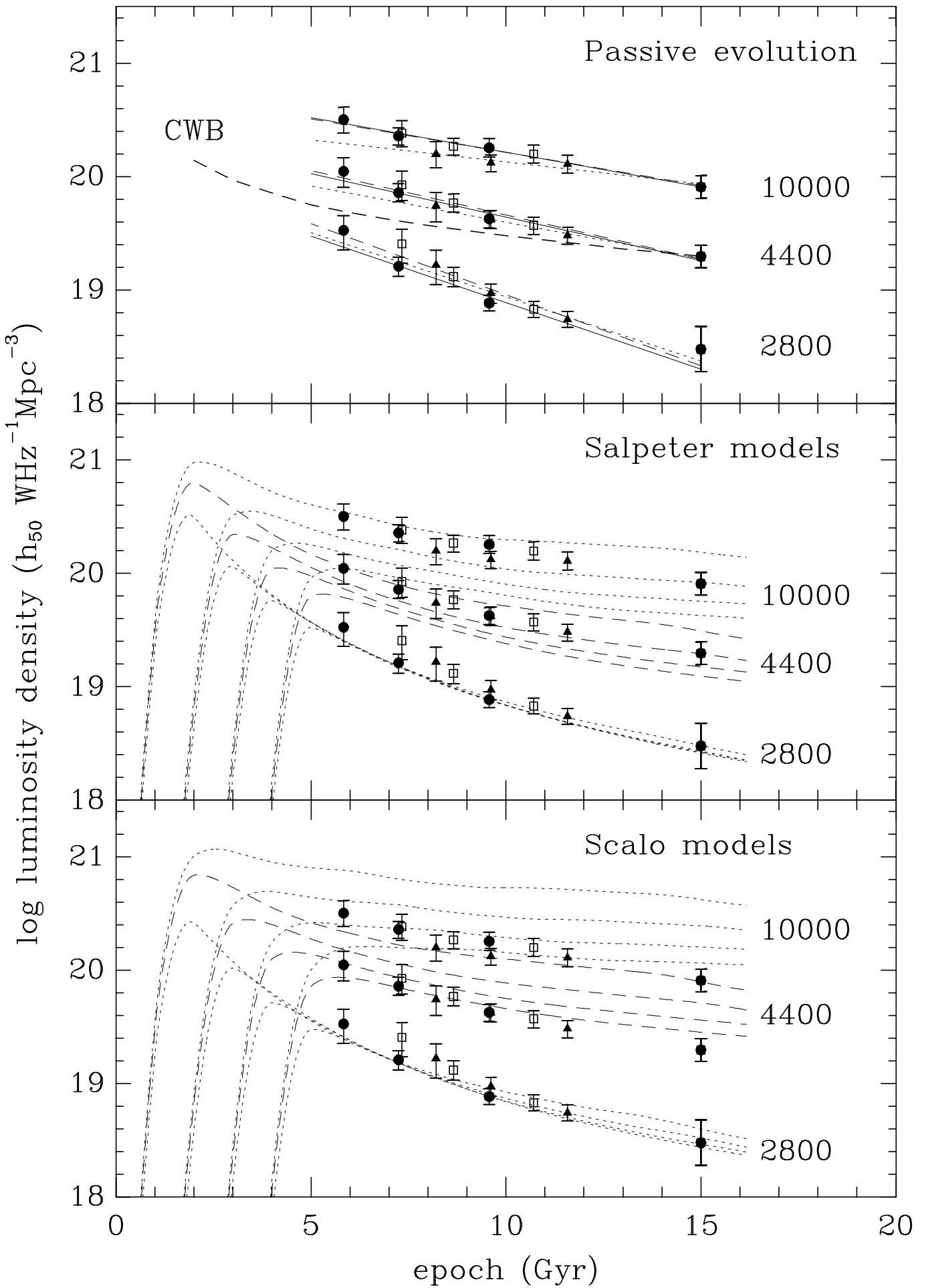


TABLE 2
ESTIMATES OF THE RATE OF EVOLUTION OF THE LUMINOSITY DENSITY

model	2800 Å ^a	4400 Å ^a	1 μm ^a	(2800 – 4400) _{15,AB} ^b	(4400 – 10000) _{15,AB} ^b
Data (0.5,1.0)	0.117±0.023	0.077±0.015	0.061±0.014	2.05±0.5	1.53±0.3
Data (0.05,0.1)	0.125±0.027	0.078±0.018	0.059±0.017	2.05±0.5	1.53±0.3
Data (-0.85,0.1)	0.113±0.030	0.064±0.020	0.039±0.020	2.05±0.5	1.53±0.3
CWB passive model	...	0.042	0.035 ^c
Scalo 3 Gyr model	0.110	0.053	0.033	3.07	1.65
Salpeter 3 Gyr model	0.110	0.070	0.043	2.22	1.62

^a $d(\log L)/dt$ in units of Gyr^{-1}

^bAB color at $z = 0$ or at an age of 15 Gyrs

^cgeometric mean of evolution in B and K